SciMedCentral

Journal of Radiology & Radiation therapy

Research Article

Normal Values of Myocardial Blood Flow and Myocardial Flow Reserve Evaluated by 3-Dimensional Dynamic PET/CT System with ^{13}N-Ammonia

Keisuke Kiso[1,2], Eku Shimosegawa[1], Hiroshi Watabe[3,4], Yasukazu Kanai[3], Koichi Fujino[1] and Jun Hatazawa[1]*

[1]*Department of Nuclear Medicine and Tracer Kinetics, Osaka University Graduate School of Medicine, Japan*
[2]*Department of Radiology, National Cerebral and Cardiovascular Center, Japan*
[3]*Department of Molecular Imaging in Medicine, Osaka University Graduate School of Medicine, Japan*
[4]*Division of Radiation Protection and Safety Control, Cyclotron and Radioisotope Center, Tohoku University, 6-3 Aramaki Aza Aoba, Aoba-ku, Sendai, Miyagi, Japan*

Corresponding author
Keisuke Kiso Department of Radiology, National Cerebral and Cardiovascular Center, 5-7-1 Fujishirodai, Suita, Osaka 565-8565, Japan, Tel: +81-6-6833-5012; Fax: +81-6-6872-7486; E-mail: kkeisuke@ncvc.go.jp

Submitted: 21 October 2013

Accepted: 14 November 2013

Published: 19 November 2013

Keywords
- ^{13}N-ammonia
- Normal values
- Myocardial blood flow
- Myocardial flow reserve

Abstract

Purpose: For quantitation of myocardial blood flow (MBF), 2-dimensional (2D) ^{13}N-ammonia PET has been utilized. However, most of recent PET systems operate only 3-dimensional (3D) mode, and there are no reports about normal value of MBF measured by 3D PET/CT system. In this study, we evaluated normal values of MBF and myocardial flow reserve (MFR) with ^{13}N-ammonia by using 3D PET/CT system. Comparisons of values between the present study and previously reports with 2D PET systems were carried out.

Materials and methods: Nine normal volunteers were enrolled. MBF of dipyridamole stress and rest were measured by 3D PET/CT with ^{13}N-ammonia. MBF was measured by 2-compartmet model analysis, and MFR was determined as the ratio of dipyridamole/rest MBF. Finally, we assessed regional (three coronary territories) and global MBF and MFR.

Results: Average MBF at dipyridamole/rest were LAD:3.42 ± 0.73/1.26 ± 0.22, LCX:4.23 ± 1.17/1.20 ± 0.22, RCA:3.68 ± 0.89/1.35 ± 0.82, global:3.69 ± 0.83/1.26 ± 0.31 (mL/min/g), respectively. Average MFR was LAD: 2.74 ± 0.43, LCX:3.54 ± 0.72, RCA:3.20 ± 1.22, global:2.98 ± 0.59, respectively. Those results were almost similar with previous reports with 2D ^{13}N-ammonia PET. However, higher rest MBF and heterogeneity of hyperemic MBF were observed.

Conclusions: Normal values of MBF and MFR with 3D ^{13}N-ammonia PET were almost comparable with the values evaluated by conventional 2D PET. However, it needs further considerations to improve heterogeneity of hyperemic MBF and higher rest MBF.

INTRODUCTION

For quantitative measurement of myocardial blood flow (MBF) and myocardial flow reserve (MFR), 2-dimensional (2D) dynamic PET with ^{13}N-ammonia has been well established [1-4]. And this noninvasive approach has been utilized for the assessment of severity of coronary artery disease [5-8] and other heart diseases [9-11], and it has also been applied for the evaluation of pharmacologic intervention [12], endothelial functions of coronary artery [13,14], and the status of myocardial microcirculation [15,16].

However, most of recent PET and PET/CT systems operate only 3-dimensional (3D) mode for the reduction of radiation dose and the improvement of sensitivity and image quality. In clinical settings, the use of 3D PET has demonstrated advantages for brain imaging [17,18] and oncology [19]. On the other hand, improvement of count rate in the 3D acquisition influences the increase of scatter, random events and dead time, compared with conventional 2D acquisition. Consequently, cardiac applications have been less clear, especially in the quantitative analysis of MBF. Moreover, there has been no report revealing about the normal values of MBF and MFR measured by 3D PET/CT system with ^{13}N-ammonia. And the comparison reports with previously reported results evaluated by conventional 2D PET system have not also been published.

In this study, we measured the normal values of MBF and MFR with ^{13}N-ammonia by using 3D PET/CT system, and investigated feasibility of 3D PET for ^{13}N-ammonia study compared with

previously reported normal values evaluated by conventional 2D dynamic PET.

MATERIALS AND METHODS

Study Population

Nine healthy volunteers (mean age: 30.3±8.7 years, 4 men) with a low likelihood of coronary artery disease were enrolled in this study. None of participants had any smoking histories, and were taking any medications. All subjects refrained from caffeine intake 24 hours prior to this PET study. This study protocol was approved by ethical committee of our university, and all subjects gave written informed consent.

PET scanner

Image data were obtained with an integrated PET/CT system (Gemini GXL, Philips co.). This PET/CT system combines the 16-slice CT scanner and a multiring gadolinium oxyorthosilicate zirconium (GSO-Zr) detector system and can acquire data in only 3D mode. The dimensions of GSO crystals are 4mm (transaxial) ×6mm (axial) ×30mm (radial). This PET/CT system has 420 photomultipliers and those detectors are arranged with PIXELAR system, not the conventional block system, for the improvement of uniformity. It covers an axial field of view (FOV) of 18cm and a transverse FOV of 57cm, and the energy window was set to 419-590 keV, and coincidence time window was set to 7.5 ns. The axial special resolution was 5.3 mm with full-width at half-maximum at 1 cm radius from the center, and the sensitivity was 8.0 cps/kBq at 10cm radius from the center. The upper limit of radioactivity concentration for this camera, as the index of the count-rate characteristic, was 17.6 kBq/mL. Detailed National Electrical Manufacturers Association NU 2-2001 performance of this PET/CT system was reported previously by Sathiakumar C, et al. [20]

Dynamic scan acquisition protocol

Regional MBF at rest and during pharmacological stress were measured as shown in Figure 1. In each MBF measurement, after CT scan for attenuation correction (120KV, 50-100mAs; auto exposure control), 185 MBq of ^{13}N-ammonia was administered with intravenous bolus injection, and immediately followed by total 12-min dynamic emission scan with list mode. The list data were sorted to following sequence of frames: 10 sec. ×12 frames + 600 sec. × 1 frame. The last frame of data was utilized for static imaging of myocardial distribution of ^{13}N-ammonia. Based on the estimation of count-rate characteristic, the dose of ^{13}N-ammonia: 185MBq was arbitrarily decided for the adequate count acquisition under the upper limit of count-rate characteristic. We took 60 minutes for the allowance of the decay of ^{13}N-ammonia

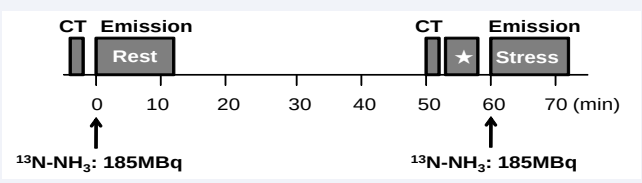

Figure 1 Dynamic scan acquisition protocol 13N-NH3 : 13N-ammonia. ☆: Dipyridamole (0.56mg/kg) infusion for 4 min.

between rest and pharmacological stress acquisitions. As the pharmacological stress to gain hyperemic state, dipyridamole (0.16mg/kg) was administrated for 4 minutes, and 3 minutes after the termination of dipyridamle infusion, ^{13}N-ammonia injection and data acquisition were started, as described above.

During the dipyridamole stress and during 15 minutes of recovery, blood pressure and heart rate were recorded every 2 minutes. Electrocardiogram (ECG) was monitored continuously throughout the dipyridamole stress, and a 12-lead ECG was recorded at baseline and every minute. At the end of PET study, 60mg of aminophylline was administrated for the reverse of dipyridamole effect.

Image reconstruction

The data were corrected for random coincidences, geometry, normalization, dead-time losses, scatter, and attenuation. The attenuation correction was performed using the attenuation map generated from CT data acquired prior to the emission scan. Scatter correction was included in the reconstruction process using "single scatter simulation method" implemented by manufacturer. The 3D emission data was reconstructed by use of line of response (LOR) algorithm without converting into 2D data set [21]. Reconstructed image had a matrix size of 128×128×52 with 4mm cubic voxel.

Data analysis

All images were transferred to an off-line personal computer (Endeavor MT8800, EPSON co. Operating system: Windows XP professional), and measurement of MBF was processed semi automatically with PMOD software package (version 2.95, PMOD Technologies Ltd.), based on the 2-compartmet model analysis as previously reported [22-24]. Regions of interest (ROI) were drawn semi automatically by use of a center-line within the myocardium in the projection of three dimensions (short-axis, vertical long, horizontal-long). According to the recommendation of American heart Association (AHA), 17-myocardial segment model was adopted for this analysis. For the input function, ROI was drawn in left ventricular blood pool, and for the septal spillover correction, ROI was drawn in right ventricular blood pool using summed data of first 0-120 seconds frames. MBF was estimated by model fitting of the myocardial time-activity curves [25]. Partial volume and spillover were corrected with the method which was developed and validated by Hutchins et al. [1,26] MFR was determined as the ratio of MBF during dipyridamole stress to that at rest. Finally, we assessed regional (LAD, LCX, and RCA territories) and global MBF and MFR.

Statistical analysis

Statistical analysis was performed with StatView statistical package (SAS Institute, Cary, NC). All data were expressed as the mean ± standard deviation. We adopted a paired *t* test for the comparison of hemodynamic findings at rest and those on dipyridamole stress, and adopted one factor repeated measures analysis of variance (ANOVA) for the analysis of MBF and MFR between three coronary territories, followed by Scheffe test if significant differences were observed. A value of $p<0.05$ was considered significant.

RESULTS

Characteristics of study subjects

Subjects' characteristics are shown in Table 1. Average age was 30.3 ± 8.7 years, average BMI was 22.2 ± 3.4. Three subjects had risk factors, two had familial history of coronary artery disease (CAD) and the other had hyperlipidemia (no need for medical therapy).

Hemodynamic changes during pharmacological stress

Hemodynamic findings such as blood pressure (systolic, diastolic, and mean pressure), heart rate, rate pressure product (RPP), were shown in Table 2. Significant increase of RPP which was observed during pharmacological stress implied that adequate vasodilation and hyperemia was achieved by dipyridamole.

Image analysis of myocardial perfusion

Visual evaluation and polar map analysis of the myocardial ^{13}N-ammonia distribution at rest and during dipyridamole hyperemia showed homogeneous uptake in all study subjects. These results suggested that all subjects were free from significant coronary artery disease. Figure 2 showed representative data in this study subjects.

Myocardial blood flow

Myocardial blood flow (MBF; mL/g/min) at rest and during dipyridamole stress of each study subject is shown in table 3. Average resting MBF was 1.26±0.22 (range: 0.88-1.56) on LAD, 1.20±0.22 (range: 0.88-1.50) on LCX, 1.35±0.82 (range: 0.76-3.39) on RCA regions, and 1.26±0.31 (range: 0.97-1.90) as global MBF. In the resting MBF, no significant difference was observed between MBF in three coronary territories. On the other hand, average blood flow on pharmacological stress was 3.42±0.73 (range: 2.49-4.28) on LAD, 4.23±1.17 (range: 2.97-6.22) on LCX, 3.68±0.89 (range: 2.34-4.92) on RCA regions, and 3.69±0.83 (range: 2.56-5.12) as global MBF. In MBF during dipyridamole stress, LCX region showed significant higher MBF than LAD region (P<0.01).

Table 1: Clinical characteristics of study subjects (n=9).

Age (years)	30.3±8.7
Height (cm)	163.3±6.1
Body wight (kg)	59.3±10.3
BMI (kg/m^2)	22.2±3.4
Risk factors (n)	familial history (2)
	hyperlipidemia (1)

Data are expressed as mean ± SD. BMI: body mass index.

Table 2: Hemodynamic findings.

	Rest	Dip.
SBP (mmHg)	96.1±12.5	95.1±14.0
DBP (mmHg)	45.0±3.7	46.8±5.8
mBP (mmHg)	62.0±5.7	62.9±7.4
HR (bpm)	61.1±7.0	90.3±8.6#
RPP (bpm·mmHg)	5852±804	8631±1805*
% increase in RPP		47.7±22.9

SBP: Systolic blood pressure; DBP: diastolic blood pressure; mBP: mean blood pressure; HR: heart rate; Bpm: beats per minute; RPP: rate pressure product. #P<0.001, *P<0.0001 vs. Rest

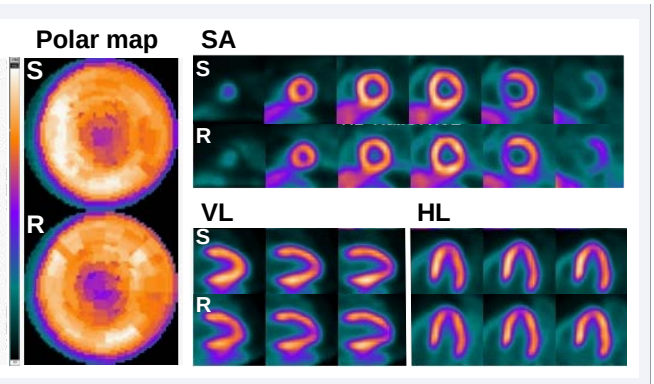

Figure 2 Representative data of 13N-ammonia distribution. Stress images are shown in upper rows and rest images are shown in lower rows. SA: short axis; VL: vertical long axis; HL: horizontal long axis; S (white letter): stress; R (white letter): rest.

Myocardial flow reserve

Myocardial flow reserve (MFR) of each study subject, which was defined as a ratio of MBF during pharmacological stress to flow at rest, was shown in table 4.

Since MBF of LCX region on dipyridamole stress was significantly higher, MFR of LCX was tending to be higher than other coronary territories; however, there was not statistical significance.

Comparison with previously reported values of MBF and MFR obtained by 2D PET systems (Table 5)

Some previous studies quantifying MBF and MFR in normal volunteers, which was evaluated by conventional 2-dimension acquisition with ^{13}N-ammonia PET (2D ammonia PET), have been reported [1,6,13-16,27,28]. Although mean global MBF at pharmacological stress was within the range of previously reported values, mean MBF at resting state showed higher trend compared to that obtained by 2D ammonia PET. Calculated MFR showed lower trend compared to the reported values.

DISCUSSION

We performed quantitative analysis of myocardial perfusion in nine healthy volunteers with ^{13}N-ammonia by using 3D PET/CT system. For the calculation of MBF, we adopted 2-compartment model analysis and utilized PMOD software. Most of the values of MBF and MFR evaluated by 3D mode were almost similar with those which were previously reported with conventional 2D mode. Some reports revealed the equivalence between 2D and 3D acquisition for the quantification of MBF with 3D/2D hybrid PET system [29-33]. Schepis T, et al. reported the comparability of 3D and 2D acquisition of ^{13}N-ammonia PET in the patients with known or suspected CAD evaluated by 3D/2D hybrid PET/CT system, for the detection of coronary artery disease with advantage of reduction for radiation exposure [33]. However, normal values of MBF absolutely quantitated with 3D PET/CT

Table 3: Myocardial blood flow (mL/g/min).

Pt.No.	LAD		LCX		RCA		Global	
	Dip.	Rest	Dip.	Rest	Dip.	Rest	Dip.	Rest
1	2.49	1.08	2.97	0.88	2.34	1.01	2.57	1.01
2	2.83	1.21	3.49	0.90	2.99	0.76	3.04	1.00
3	3.05	1.10	3.38	1.32	3.34	1.15	3.21	1.17
4	3.02	0.88	4.45	1.11	4.31	0.99	3.73	0.97
5	3.48	1.56	4.24	1.50	4.23	1.10	3.88	1.42
6	4.28	1.45	6.22	1.28	4.08	1.84	4.72	1.51
7	3.09	1.17	3.43	1.15	2.62	0.93	3.04	1.09
8	4.74	1.44	6.02	1.49	4.92	0.95	5.12	1.31
9	3.76	1.41	3.83	1.15	4.32	3.39	3.93	1.90
mean	3.42	1.26	4.23*	1.20	3.68	1.35	3.69	1.26
SD	0.73	0.22	1.17	0.22	0.89	0.82	0.83	0.31

Pt.No.: patients' number, LAD: left anterior descending coronary artery, LCX: left circumflex coronary artery, RCA: right coronary artery
*P<0.01 vs. LAD

Table 4: Myocardial flow reserve.

Pt. No.	LAD	LCX	RCA	Global
1	2.31	3.37	2.31	2.54
2	2.33	3.87	3.93	3.04
3	2.77	2.56	2.90	2.74
4	3.43	4.00	4.35	3.84
5	2.23	2.82	3.84	2.73
6	2.95	4.85	2.21	3.12
7	2.64	2.98	2.81	2.78
8	3.29	4.04	5.17	3.90
9	2.66	3.33	1.27	2.06
mean	2.74	3.54	3.20	2.98
SD	0.43	0.72	1.22	0.59

LAD: left anterior descending coronary artery, LCX: left circumflex coronary artery, RCA: right coronary artery.

Table 5: Comparison with previously reported values of global MBF and MFR.

	MBF (mL/g/min)		MFR	mode	PET system	kinetic model	Author
	stress	rest					
★	3.69±0.83	1.26±0.31	2.98±0.59	3D	Philips Gemini GXL	2-compartment	this study
1	4.3±1.3	1.1±0.2	4.0±1.3	2D	CTI/Siemens 931/8	NA	Chan et al. [28]
2	2.04±0.47	0.68±0.14	3.06±0.58	2D	CTI ECAT-EXACT	2-compartment	Campisi et al. [13,27]
3	2.85±0.49	0.67±0.11	4.28±0.62	2D	Siemens 931	3-compartment	Muzik et al. [6]
4	3.27±0.43	0.86±0.14	3.88±0.70	2D	CTI/Siemens EXACT HR	3-compartment	Di Carli et al. [14]
5	2.62±1.20	0.73±0.17	3.80±1.00	2D	shimadu headtome 4	2-compartment	Yokoyama I, et al [15]
6	3.22±1.74	0.75±0.35	4.22±1.42	2D	shimadu headtome 4	2-compartment	Yokoyama et al. [16]
7	4.17±1.11	0.88±0.17	4.80±1.3	2D	CTI ECAT-911	3-compartment	Huchins et al. [1]

MBF=myocardial blood flow, MFR= myocardial flow reserve, NA: not available
[ ] = reference number.

system have not been reported. Schepis T, et al. showed good agreements between MBF values obtained by 3D acquisition and 2D acquisition. There are discrepancies between our results and theirs. For examples, the average MBF values at rest and those on stress of this study were higher, and MFR was lower. These discrepancies might be due to different study conditions: 1. physical differences of PET/CT systems (numbers of rings and crystals of PET detectors), 2. Reconstruction methods (2D-FBP/3D-FORE-FBP/3D-FORE-OSEM/3D-RIP vs. 3D-LOR), 3. Study subjects (suspected or known coronary artery diseases vs. normal healthy subjects), 4. Analyzed time duration of dynamic data (20-min vs. 2-min). For example, since each PET system has different numbers of rings and materials of detectors, the influences of scatter, random event, and dead time were different, MBF measurement by 3D PET/CT system has not been generally authorized for quantitative accuracy. In this study, since our PET/

CT system has only availability of 3D data acquisition and was unable to make direct comparison between 2D and 3D data in the same system, we surveyed the previously reported data obtained by 2D acquisition data and compared with the present results. Although MBF at pharmacological stress matched with that by 2D acquisition data, higher MBF at rest and regional heterogeneity in MBF on pharmacological stress were observed, which were different from data previously reported.

Some reasons for higher MBF at rest are speculated. One is the lower dose of ^{13}N-ammonia; 185 MBq than other studies. The lowest dose of ^{13}N-ammonia in previous reports was 500 MBq [33]. In this study, based on the evaluation of count-rate characteristic of this PET/CT system, dose of ^{13}N-ammonia: 185 MBq was determined. However, lower dose than previous studies might induce susceptibility to noises and image quality. Since the compartment analysis for ^{13}N-ammonia utilizes image-driven arterial input function, the noises on both myocaridial tissue and input function cause bias in the estimated MBF value, especially in lower myocardial perfusion state like at rest. The other was that scatter correction in 3D mode might be insufficient for the quantitative analysis. In 3D mode, scatter event are typically 30% to 50% of the total collected counts [34]. Therefore, 3D acquisition needs appropriate correction method for scatter. In this PET/CT system, single scatter simulation method was included in the reconstruction process, and this method reported to yield images with quantitative accuracy [35]. However, in theory, single scatter simulation cannot handle the multiple scatter and the scatter originating from outside the FOV of the scanner. Furthermore, since single scatter simulation is performed with extremely complicated algorithm, the cases which were included error data, such as misalignment of CT attenuation correction (CTAC) map and emission PET data, would be influenced by significant artifacts [34]. For these reasons, scatter correction with this method might be insufficient for the myocardial blood flow analysis, especially at rest state which showed lower blood flow and might be susceptible to scatters.

There were few reports describing about the uniformity of regional MBF in normal subjects evaluated by 2D ammonia PET. Nagamachi S, et al. reported the normal values of regional MBF at rest and during pharmacological stress: LAD (stress/rest) = 1.93±0.39/0.59±0.13, LCX (stress/rest) =1.95±0.43/0.65±0.21, RCA (stress/rest) =2.14±0.43/0.64±0.14 (mL/g/min), and they concluded that no heterogeneity was observed in MBF of three coronary territories in both rest and stress state [36]. And Hutshins GD, et al. also reported that there was no heterogeneity in MBF of each coronary arteries (values of MBF were not available in the text) [1]. However, this study showed different results from previous reports, that heterogeneity of MBF during pharmacological stress was observed: MBF during pharmacological stress on LCX was higher than that on LAD territory.

Misalignment between CTAC map and PET images was thought to be one of the factors for influencing to the heterogeneity in our study. Koepfli, et al. reported that CTAC was comparable to conventional transmission scan with a rotating Ge-68 source for the qualitative and quantitative assessment of MBF [37]. However, Alessio, et al. revealed that helical CT was insufficient for the attenuation correction of cardiac PET, because respiratory motion induced misalignment of the attenuation map and emission PET images. And they concluded that cine CT would offer an alternative to helical CT for compensating for respiratory motion in the attenuation correction [38]. Furthermore, Loghin, et al. demonstrated in conventional rest/stress PET studies, 21.7% of the studies showed misalignment artifact typically in anterolateral or lateral segments of the left ventricle. Through manual corregistration of transmission and emission data, the artifacts could be removed [39]. In this study, helical CT was utilized as a tool for attenuation correction. We performed automatic coregistration between CT and PET image with manual adjustment. In a visual evaluation, it was difficult to detect major misalignment. However, minor misalignment which could not be detected by visual evaluation might be present and gave some influences to the heterogeneity. Moreover, as the other reason for these results, scatter correction in 3D mode, which was similar with the reason of higher MBF at rest described above, might be insufficient to eliminate the regional heterogeneity.

There were several limitations in this study. As previously described, direct comparison between values evaluated by 2D and 3D mode was impossible in this PET/CT system. Therefore, we could not conclude about the absolute equivalence of this PET/CT system and conventional 2D acquisition. Furthermore, since this study dealt with a small number of subjects, these results need to be confirmed in larger study for statistically certain analysis.

CONCLUSIONS

We performed quantitative measurement of normal value of MBF and MFR with ^{13}N-ammonia by using 3D PET/CT system, and those results were almost comparable with the values measured by conventional 2D PET system. However, higher rest MBF and heterogeneity of hyperemic MBF was observed. Therefore, for more accurate evaluation of MBF and MFR by using 3D PET/CT system, the improvement of the alignment of CTAC map and PET images, scatter correction, and the consideration of dose of [13] N-ammonia administration might be necessary.

REFERENCES

1. Hutchins GD, Schwaiger M, Rosenspire KC, Krivokapich J, Schelbert H, Kuhl DE. Noninvasive quantification of regional blood flow in the human heart using N-13 ammonia and dynamic positron emission tomographic imaging. J Am Coll Cardiol. 1990; 15: 1032-1042.

2. Kuhle WG, Porenta G, Huang SC, Buxton D, Gambhir SS, Hansen H, et al. Quantification of regional myocardial blood flow using 13N-ammonia and reoriented dynamic positron emission tomographic imaging. Circulation. 1992; 86: 1004-1017.

3. Okazawa H, Takahashi M, Hata T, Sugimoto K, Kishibe Y, Tsuji T. Quantitative evaluation of myocardial blood flow and ejection fraction with a single dose of (13)NH(3) and Gated PET. J Nucl Med. 2002; 43: 999-1005.

4. Schelbert HR, Phelps ME, Huang SC, MacDonald NS, Hansen H, Selin C, et al. N-13 ammonia as an indicator of myocardial blood flow. Circulation. 1981; 63: 1259-1272.

5. Gewirtz H, Skopicki HA, Abraham SA, Castano H, Dinsmore RE, Alpert NM, et al. Quantitative PET measurements of regional myocardial blood flow: observations in humans with ischemic heart disease. Cardiology. 1997; 88: 62-70.

6. Muzik O, Duvernoy C, Beanlands RS, Sawada S, Dayanikli F, Wolfe ER, Jr. et al. Assessment of diagnostic performance of quantitative flow measurements in normal subjects and patients with angiographically documented coronary artery disease by means of nitrogen-13 ammonia and positron emission tomography. J Am Coll Cardiol. 1998; 31: 534-40.

7. Schelbert HR, Wisenberg G, Phelps ME, Gould KL, Henze E, Hoffman EJ, et al. Noninvasive assessment of coronary stenoses by myocardial imaging during pharmacologic coronary vasodilation. VI. Detection of coronary artery disease in human beings with intravenous N-13 ammonia and positron computed tomography. Am J Cardiol. 1982; 49: 1197-1207.

8. Tamaki N, Yonekura Y, Senda M, Kureshi SA, Saji H, Kodama S, et al. Myocardial positron computed tomography with 13N-ammonia at rest and during exercise. Eur J Nucl Med. 1985; 11: 246-251.

9. Cecchi F, Olivotto I, Gistri R, Lorenzoni R, Chiriatti G, Camici PG. Coronary microvascular dysfunction and prognosis in hypertrophic cardiomyopathy. N Engl J Med. 2003; 349: 1027-1035.

10. Neglia D, Michelassi C, Trivieri MG, Sambuceti G, Giorgetti A, Pratali L, et al. Prognostic role of myocardial blood flow impairment in idiopathic left ventricular dysfunction. Circulation. 2002; 105: 186-193.

11. Tadamura E, Yoshibayashi M, Yonemura T, Kudoh T, Kubo S, Motooka M, et al. Significant regional heterogeneity of coronary flow reserve in paediatric hypertrophic cardiomyopathy. Eur J Nucl Med. 2000; 27: 1340-1348.

12. Guethlin M, Kasel AM, Coppenrath K, Ziegler S, Delius W, Schwaiger M. Delayed response of myocardial flow reserve to lipid-lowering therapy with fluvastatin. Circulation. 1999; 99: 475-481.

13. Campisi R, Czernin J, Schöder H, Sayre JW, Marengo FD, Phelps ME, et al. Effects of long-term smoking on myocardial blood flow, coronary vasomotion, and vasodilator capacity. Circulation. 1998; 98: 119-125.

14. Di Carli MF, Janisse J, Grunberger G, Ager J. Role of chronic hyperglycemia in the pathogenesis of coronary microvascular dysfunction in diabetes. J Am Coll Cardiol. 2003; 41: 1387-1393.

15. Yokoyama I, Momomura S, Ohtake T, Yonekura K, Nishikawa J, Sasaki Y, et al. Reduced myocardial flow reserve in non-insulin-dependent diabetes mellitus. J Am Coll Cardiol. 1997; 30: 1472-1477.

16. Yokoyama I, Ohtake T, Momomura S, Nishikawa J, Sasaki Y, Omata M. Reduced coronary flow reserve in hypercholesterolemic patients without overt coronary stenosis. Circulation. 1996; 94: 3232-3238.

17. Cherry SR, Woods RP, Hoffman EJ, Mazziotta JC. Improved detection of focal cerebral blood flow changes using three-dimensional positron emission tomography. J Cereb Blood Flow Metab. 1993; 13: 630-638.

18. Sadato N, Carson RE, Daube-Witherspoon ME, Campbell G, Hallett M, Herscovitch P. Optimization of noninvasive activation studies with 15O-water and three-dimensional positron emission tomography. J Cereb Blood Flow Metab. 1997; 17: 732-739.

19. Lodge MA, Badawi RD, Gilbert R, Dibos PE, Line BR. Comparison of 2-dimensional and 3-dimensional acquisition for 18F-FDG PET oncology studies performed on an LSO-based scanner. J Nucl Med. 2006; 47: 23-31.

20. Sathiakumar C, Som S, Eberl S, Lin P. NEMA NU 2-2001 performance testing of a Philips Gemini GXL PET/CT scanner. Australas Phys Eng Sci Med. 2010; 33: 199-209.

21. adrmas DJ. LOR-OSEM: statistical PET reconstruction from raw line-of-response histograms. Phys Med Biol. 2004; 49: 4731-4744.

22. Koepfli P, Wyss CA, Namdar M, Klainguti M, von Schulthess GK, Lüscher TF, et al. Beta-adrenergic blockade and myocardial perfusion in coronary artery disease: differential effects in stenotic versus remote myocardial segments. J Nucl Med. 2004; 45: 1626-1631.

23. Namdar M, Koepfli P, Grathwohl R, Siegrist PT, Klainguti M, Schepis T, et al. Caffeine decreases exercise-induced myocardial flow reserve. J Am Coll Cardiol. 2006; 47: 405-410.

24. Wyss CA, Koepfli P, Mikolajczyk K, Burger C, von Schulthess GK, Kaufmann PA. Bicycle exercise stress in PET for assessment of coronary flow reserve: repeatability and comparison with adenosine stress. J Nucl Med. 2003; 44: 146-154.

25. DeGrado TR, Hanson MW, Turkington TG, Delong DM, Brezinski DA, Vallée JP, et al. Estimation of myocardial blood flow for longitudinal studies with 13N-labeled ammonia and positron emission tomography. J Nucl Cardiol. 1996; 3: 494-507.

26. Hutchins GD, Caraher JM, Raylman RR. A region of interest strategy for minimizing resolution distortions in quantitative myocardial PET studies. J Nucl Med. 1992; 33: 1243-1250.

27. Campisi R, Czernin J, Karpman HL, Schelbert HR. Coronary vasodilatory capacity and flow reserve in normal myocardium supplied by bypass grafts late after surgery. Am J Cardiol. 1997; 80: 27-31.

28. Chan SY, Brunken RC, Czernin J, Porenta G, Kuhle W, Krivokapich J, et al. Comparison of maximal myocardial blood flow during adenosine infusion with that of intravenous dipyridamole in normal men. J Am Coll Cardiol. 1992; 20: 979-985.

29. deKemp RA, Yoshinaga K, Beanlands RS. Will 3-dimensional PET-CT enable the routine quantification of myocardial blood flow? J Nucl Cardiol. 2007; 14: 380-397.

30. Knesaurek K, Machac J, Krynyckyi BR, Almeida OD. Comparison of 2-dimensional and 3-dimensional 82Rb myocardial perfusion PET imaging. J Nucl Med. 2003; 44: 1350-1356.

31. Lekx KS, deKemp RA, Beanlands RS, Wisenberg G, Wells G, Stodilka RZ, et al. 3D versus 2D dynamic 82Rb myocardial blood flow imaging in a canine model of stunned and infarcted myocardium. Nucl Med Commun. 31: 75-81.

32. Roelants V, Bol A, Bernard X, Coppens A, Melin J, Gerber B, et al. Direct comparison between 2-dimensional and 3-dimensional PET acquisition modes for myocardial blood flow absolute quantification with O-15 water and N-13 ammonia. J Nucl Cardiol. 2006; 13: 220-224.

33. Schepis T, Gaemperli O, Treyer V, Valenta I, Burger C, Koepfli P, et al. Absolute quantification of myocardial blood flow with 13N-ammonia and 3-dimensional PET. J Nucl Med. 2007; 48: 1783-1789.

34. Accorsi R, Adam LE, Werner ME, Karp JS. Optimization of a fully 3D single scatter simulation algorithm for 3D PET. Phys Med Biol. 2004; 49: 2577-2598.

35. Ollinger JM. Model-based scatter correction for fully 3D PET. Phys Med Biol. 1996; 41: 153-176.

36. Nagamachi S, Czernin J, Kim AS, Sun KT, Böttcher M, Phelps ME, et al.

Reproducibility of measurements of regional resting and hyperemic myocardial blood flow assessed with PET. J Nucl Med. 1996; 37: 1626-1631.

37. Koepfli P, Hany TF, Wyss CA, Namdar M, Burger C, Konstantinidis AV, et al. CT attenuation correction for myocardial perfusion quantification using a PET/CT hybrid scanner. J Nucl Med. 2004; 45: 537-542.

38. Alessio AM, Kohlmyer S, Branch K, Chen G, Caldwell J, Kinahan P. Cine CT for attenuation correction in cardiac PET/CT. J Nucl Med. 2007; 48: 794-801.

39. Loghin C, Sdringola S, Gould KL. Common artifacts in PET myocardial perfusion images due to attenuation-emission misregistration: clinical significance, causes, and solutions. J Nucl Med. 2004; 45: 1029-1039.

Cite this article

Kiso K, Shimosegawa E, Watabe H, Kanai Y, Fujino K, et al. (2013) Normal Values of Myocardial Blood Flow and Myocardial Flow Reserve Evaluated by 3-Dimensional Dynamic PET/CT System with ^{13}N-Ammonia. J Radiol Radiat Ther 1(3): 1016.